

Equation A7 can be integrated by considering the HN_3 concentration constant. The result is

$$\ln \frac{(\text{N}_2\text{H}_4)}{(\text{N}_2\text{H}_4)_0} = -nFt \quad (\text{A8})$$

where

$$n = \frac{2k_4(\text{HN}_3) + 3k_5'(\text{NO}_3^-)}{k_4(\text{HN}_3) + k_5'(\text{NO}_3^-)}$$

The rate law for NH_4^+ from reaction 4 is

$$d(\text{NH}_4^+)/dt = k_4(\text{HN}_3)(\text{H}^+)(\text{N}_2\text{H}_2) \quad (\text{A9})$$

Substituting from eq A4 for (N_2H_2) gives

$$d(\text{NH}_4^+)/dt = \frac{k_4(\text{HN}_3)(\text{N}_2\text{H}_4)F}{k_4(\text{HN}_3) + k_5'(\text{NO}_3^-)} \quad (\text{A10})$$

(N_2H_4) is replaced by $(\text{N}_2\text{H}_4)_0 \exp(-nFt)$, and the resulting expression is integrated. After evaluation of the integration constant, the result is

$$(\text{NH}_4^+) = \left(\frac{k_4(\text{HN}_3)}{2k_4(\text{HN}_3) + 3k_5'(\text{NO}_3^-)} \right) (\text{N}_2\text{H}_4)_0 [1 - \exp(-nFt)] \quad (\text{A11})$$

A more useful form is the equivalent expression

$$(\text{NH}_4^+) = \frac{k_4(\text{NH}_3)}{2k_4(\text{HN}_3) + 3k_5'(\text{NO}_3^-)} [(\text{N}_2\text{H}_4)_0 - (\text{N}_2\text{H}_4)_t] \quad (\text{A12})$$

where $(\text{N}_2\text{H}_4)_t$ is the N_2H_4 concentration at time t .

The rate law for HN_3 , derived from reactions 2-4, is

$$d(\text{HN}_3)/dt = [k_2'(\text{N}_2\text{H}_4)(\text{H}^+) - k_3(\text{HN}_3)](\text{HNO}_2) - k_4(\text{HN}_3)(\text{H}^+)(\text{N}_2\text{H}_2) \quad (\text{A13})$$

After equivalent expressions are substituted for HNO_2 and N_2H_2 , eq A15 becomes

$$d(\text{HN}_3)/dt = F(\text{N}_2\text{H}_4) \{ [k_2'(\text{N}_2\text{H}_4)(\text{H}^+)] [1 - k_4(\text{HN}_3)] - k_3(\text{HN}_3) [1 + k_4(\text{HN}_3)] \} / [k_2'(\text{N}_2\text{H}_4)(\text{H}^+) + k_3(\text{HN}_3)] \times [k_4(\text{HN}_3) + k_5'(\text{NO}_3^-)] \quad (\text{A14})$$

The fraction enclosed in braces will be represented below as m . The fraction m includes terms depending on HN_3 and N_2H_4 , which are mixed to the extent that the separation of variables does not appear possible. The approach taken was to assume

$$k_2'(\text{N}_2\text{H}_4)(\text{H}^+) \gg k_3(\text{HN}_3)$$

in the denominator of m . This leads, after substitution of $(\text{N}_2\text{H}_4)_0 [1 - \exp(-nFt)]$ for N_2H_4 and integration, to the expression

$$(\text{HN}_3) = \frac{[1 - k_4(\text{HN}_3)] [(\text{N}_2\text{H}_4)_0 - (\text{N}_2\text{H}_4)_t]}{2k_4(\text{HN}_3) + 3k_5'(\text{NO}_3^-)} \frac{Fk_3(\text{HN}_3) [1 + k_4(\text{HN}_3)] t}{k_2'(\text{H}^+) [k_4(\text{HN}_3) + k_5'(\text{NO}_3^-)]} \quad (\text{A15})$$

In form, eq A15 is an exponential growth combined with a linear decay, although the data would be expected to have an exponential decay. However, eq A15 does fit the data fairly well.

The rate law for N_2 from reactions 3-5 is

$$d(\text{N}_2)/dt = k_3(\text{HN}_3)(\text{HNO}_2) + [2k_4(\text{HN}_3) + k_5'(\text{NO}_3^-)](\text{H}^+)(\text{N}_2\text{H}_2) \quad (\text{A16})$$

Since the rate law for N_2O from reaction 3 is

$$d(\text{N}_2\text{O})/dt = k_3(\text{HN}_3)(\text{HNO}_2) \quad (\text{A17})$$

then

$$d(\text{N}_2)/dt = d(\text{N}_2\text{O})/dt + [2k_4(\text{HN}_3) + k_5'(\text{NO}_3^-)](\text{H}^+)(\text{N}_2\text{H}_2) \quad (\text{A18})$$

Registry No. N_2H_4 , 302-01-2; HNO_3 , 7697-37-2; Fe, 7439-89-6.

Contribution from the Department of Chemistry, University of Pittsburgh, Pittsburgh, Pennsylvania 15260

Characterization of *o*-Phenanthroline and 2,2'-Bipyridine Complexes by Laser Mass Spectrometry

K. Balasanmugam, Robert J. Day,[†] and David M. Hercules*

Received January 18, 1985

A series of *o*-phenanthroline (*o*-phen) and 2,2'-bipyridine (bpy) metal complexes has been studied by using laser mass spectrometry (LMS). The molecular cation is observed in the positive ion spectra for the tetracoordinated complexes $[\text{Ag}(\text{L})_2]\text{NO}_3$, $[\text{Cu}(\text{L})_2]\text{SO}_4 \cdot 5\text{H}_2\text{O}$, $[\text{Cu}(\text{L})_2]\text{SO}_4$, and $[\text{Tl}(\text{L})_2](\text{ClO}_4)$, where $\text{L} = \text{bpy}$ or *o*-phen. Structurally significant fragment ions (ML_2^+ , ML^+ , M^+ , LH^+) are also observed. The hexacoordinated complexes $[\text{M}(\text{L})_3]\text{Cl}_2$ and $[\text{Fe}(\text{L})_3](\text{ClO}_4)_2$, where $\text{L} = \text{bpy}$ or *o*-phen and $\text{M} = \text{Ni}$, Co , or Ru , show molecular cations in the positive ion spectra; $[\text{Mn}(\text{bpy})_3]\text{Br}_2$ does not. Generally, fragment ions such as ML_3^+ , ML_2X^+ , ML_2^+ , MLX^+ , ML^+ , and $(\text{L} + \text{H})^+$ are observed, where $\text{X} = \text{halogen}$. Complexes such as $[\text{M}(\text{o-phen})_2(\text{H}_2\text{O})_4](\text{ClO}_4)_2 \cdot 2\text{o-phen}$, where $\text{M} = \text{Ba}$ or Pb , show ions having four ligands, e.g. $\text{ML}_4\text{ClO}_4^+$. The effect of anion on the fragmentation pattern of transition-metal complexes was studied with $[\text{Ni}(\text{bpy})_3]\text{X}_2$ where $\text{X} = \text{Cl}^-$, Br^- , I^- , ClO_4^- , or SCN^- . Molecular cations were observed for all nickel complexes. The fragmentation patterns were similar for halide analogues. Ions arising from ion-molecule reactions from the dissociated products of ClO_4^- and CNS^- are observed. The negative ion LMS spectra of all complexes provide information about the anion and the formal oxidation state of the central metal atom.

Introduction

The mass spectrometry of coordination compounds is of interest because of their use in catalysis and chemical analysis.¹⁻³ Because many coordination compounds are involatile and thermally labile, analysis by mass spectrometry has been limited. Conventional mass spectrometry^{4,5} has been used with limited success; field

desorption (FD) has been applied to some inorganic complexes.⁶⁻⁹ Though fast atom bombardment (FAB) is widely used for the

- (1) Schilt, A. A. "Analytical Applications of 1,10-Phenanthroline and Related Compounds"; Pergamon Press: Oxford, England, 1969.
- (2) Hughes, M. C.; Macero, D. J. *Inorg. Chem.* **1976**, *15*, 2040-2044.
- (3) Kepert, D. L. "Inorganic Stereochemistry"; Springer-Verlag: Berlin, Heidelberg, 1982.
- (4) Indrichan, K. M.; Gerbelen, N. V. *Zh. Neorg. Khim.* **1981**, *26*, 291-301; *Russ. J. Inorg. Chem. (Engl. Transl.)* **1981**, *26*, 157-163.

[†] Present address: IBM System Products Division, Endicott, NY 13760.

Table I. 2,2'-Bipyridine and *o*-Phenanthroline Metal Complexes Studied^a

Tetracoordinate Complexes
[Ag(bpy) ₂] ₂ NO ₃ , [Cu(bpy) ₂] ₂ SO ₄ ·5H ₂ O, [Ag(<i>o</i> -phen) ₂] ₂ NO ₃ , [Cu(<i>o</i> -phen) ₂] ₂ SO ₄ ·5H ₂ O, [Ti(<i>o</i> -phen) ₂](ClO ₄) ₂
Hexacoordinate Complexes
[Ru(bpy) ₃] ₂ Cl ₂ , [Co(<i>o</i> -phen) ₃] ₂ Cl ₂ , [Fe(<i>o</i> -phen) ₃](ClO ₄) ₂ , [Ni(<i>o</i> -phen) ₃] ₂ Cl ₂ , [Mn(bpy) ₃] ₂ Br ₂ , [Fe(bpy) ₃](ClO ₄) ₂ , [Ni(bpy) ₃] ₂ X ₂ (X = Cl ⁻ , Br ⁻ , I ⁻ , NCS ⁻ , ClO ₄ ⁻)
Other Complexes
[M(<i>o</i> -phen) ₂ (H ₂ O) ₄](ClO ₄) ₂ ·2 <i>o</i> -phen (M = Ba, Pb)

^aKey: bpy, 2,2'-bipyridine; *o*-phen, *o*-phenanthroline; dmp, 2,9-dimethyl-*o*-phenanthroline. All ligands are referred to as "L" in the text.

characterization of large polar molecules, there have been few applications to coordination compounds.¹⁰⁻¹² The direct analysis of a variety of coordination compounds and organometallics by secondary ion mass spectrometry (SIMS)^{13,14} has been reported. Laser mass spectrometry (LMS) has been applied successfully to characterization of some transition-metal complexes and organometallics,^{15,16} but it has not been used extensively.

In the present work LMS has been used to investigate a series of 2,2'-bipyridine (bpy) and *o*-phenanthroline (*o*-phen) complexes; these compounds are listed in Table I. Complexes of 2,2'-bipyridine and *o*-phenanthroline with many metals frequently are involatile and thermally labile. Thus, they are ideally suited for characterization by laser mass spectrometry.

Except for one case, all complexes show intact cations in the positive ion LMS; structurally significant fragment ions are observed for all complexes. The negative ion spectra of these complexes generally are not useful for structure elucidation.

Experimental Section

Laser mass spectra were obtained by using a LAMMA 1000 laser microprobe mass spectrometer, which has been described elsewhere.¹⁷ The output of a frequency-quadrupled Q-switched Nd-YAG pulsed laser (265 nm, 15 ns pulse width) is focused (~5 μm) on the sample with a microscope objective. The laser power was varied by using a continuously variable, neutral-density filter; spectra were obtained with laser power densities of 10⁸-10⁹ W/cm². The acceleration potential was 4 keV. To obtain spectra, samples were dissolved or dispersed in methanol and deposited on a glass slide. Each spectrum presented as a figure was obtained from a single laser shot. Relative intensities reported represent an average of 10-15 shots.

The coordination compounds studied in the present investigation are listed in Table I. [Ag(*o*-phen)₂](NO₃), [Ti(*o*-phen)₂](ClO₄)₂, and [M(*o*-phen)₂(H₂O)₄](ClO₄)₂·2*o*-phen (M = Ba, Pb) were prepared and purified, as described in the literature.¹⁸ The complexes [Ru(bpy)₃]₂Cl₂ and [Fe(*o*-phen)₃](ClO₄)₂ were purchased from G. Frederick Smith Chemical Co. and used without further purification. The nickel(II) chelates

- (5) Given, K. W.; Mattson, B. M.; Miessler, G. L.; Pignolet, L. H. *J. Inorg. Nucl. Chem.* **1977**, *39*, 1309-1316.
- (6) Cerny, R. L.; Sullivan, B. P.; Bursley, M. M.; Meyer, J. T. *Anal. Chem.* **1983**, *55*, 1954-1958.
- (7) Games, D. E.; Gower, J. L.; Gower, M.; Kane-Maguire, L. A. P. *J. Organomet. Chem.* **1980**, *193*, 229-234.
- (8) Games, D. E.; Gower, J. L.; Kane-Maguire, L. A. P. *J. Chem. Soc., Dalton Trans.* **1981**, 1994-1996.
- (9) McEwen, C. N.; Ittel, S. D. *Org. Mass Spectrom.* **1980**, *15*, 35-37.
- (10) Tkatchenko, I.; Neibecker, D.; Fraisse, D.; Gomez, F.; Barofsky, D. F. *Int. J. Mass Spectrom. Ion Phys.* **1983**, *46*, 499-502.
- (11) Johnstone, R. A. W.; Lewis, I. A. S. *Int. J. Mass Spectrom. Ion Phys.* **1983**, *46*, 451-454.
- (12) Barber, M.; Bordoh, R. S.; Sedgwick, R. D.; Tyler, A. N. *Biomed. Mass Spectrom.* **1981**, *8*, 491-495.
- (13) Pierce, J. L.; Busch, K. L.; Cooks, R. G.; Walton, R. A. *Inorg. Chem.* **1983**, *22*, 2492-2494.
- (14) Pierce, J. L.; Busch, K. L.; Walton, R. A. *Organometallics* **1982**, *1*, 1328-1332.
- (15) Rohly, K. E.; Heffren, J. S.; Douglas, B. E. *Org. Mass Spectrom.* **1984**, *19*, 398-402.
- (16) Muller, J. F.; Magar, J. M.; Cagniant, D.; Mouchot, J. M.; Grimblot, J.; Bonnelle, J. G. *J. Organomet. Chem.* **1981**, *205*, 329-341.
- (17) Heinen, H. J.; Meier, S.; Vogt, H. *Springer Ser. Chem. Phys.* **1983**, *25*, 229-234.
- (18) Pfeiffer, P.; Christeleit, W. Z. *Anorg. Allg. Chem.* **1938**, *239*, 133-137.

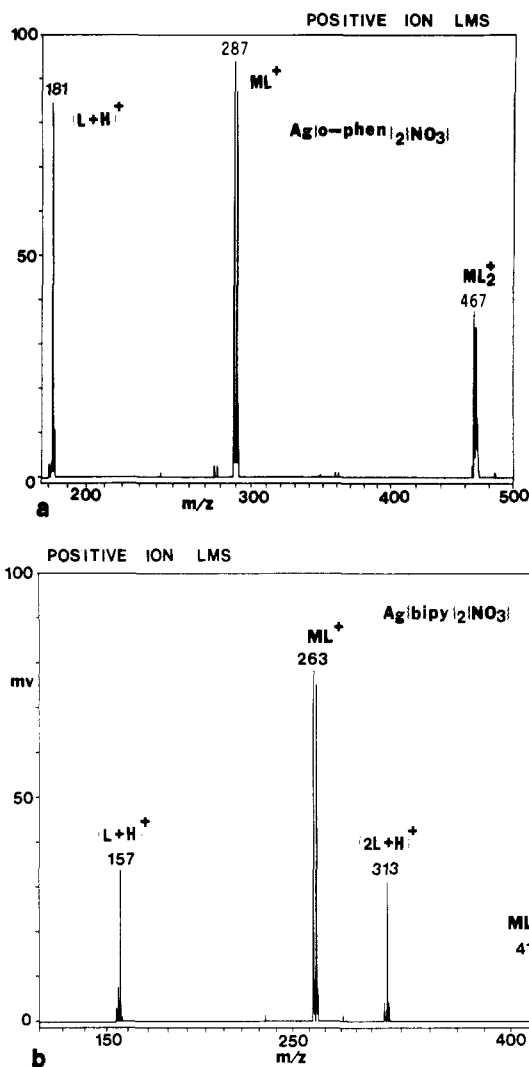


Figure 1. Positive ion laser mass spectra of [Ag(*o*-phen)₂]₂NO₃ (a) and [Ag(bpy)₂]₂NO₃ (b).

[Ni(bpy)₃]₂X₂, where X = Br⁻, I⁻, NCS⁻, and ClO₄⁻, were prepared by first synthesizing the chloride analogue¹⁹ and then substituting the chloride by appropriate anions with the use of standard methods.¹⁹ The compound [Co(*o*-phen)₃]₂Cl₂ was prepared by using a procedure¹⁹ similar to that described for [Ni(*o*-phen)₃]₂Cl₂. The copper (I, II) complexes [Cu(bpy)₂]₂SO₄,²⁰ [Cu(*o*-phen)₂]₂SO₄·5H₂O, [Cu(dmp)₂]₂SO₄·5H₂O, and the silver complex [Ag(bpy)₂]₂NO₃²¹ were prepared by the stoichiometric addition of the appropriate ligand to a solution of the metal ion. [Mn-(bpy)₃]₂Br₂ was synthesized according to the literature.²² Because all the complexes described above were synthesized and purified by using well-documented standard techniques, the authenticity and purity of the complexes were not checked by other methods.

Results

Positive Ion Spectra. Tetracoordinate Complexes. The positive ion spectra of [Ag(*o*-phen)₂]₂NO₃ and [Ag(bpy)₂]₂NO₃ are shown in Figure 1 for the mass range *m/z* > 150; results for these compounds (1-6) and other tetracoordinated complexes are summarized in Table II. The positive ion spectra of all tetra-coordinated complexes show ions corresponding to ML₂⁺, ML⁺, and (L + H)⁺ (where M = central metal atom, L = ligand) in the mass range *m/z* > 150 and only M⁺, K⁺, and Na⁺ below *m/z* = 150. Sometimes ions corresponding to (2L + H)⁺ are also observed. The positive ion spectrum of [Ti(*o*-phen)₂](ClO₄)₂ shows an ion corresponding to ML₃⁺, in addition to the ions produced

- (19) Morgan, G. T.; Burrstall, F. H. *J. Chem. Soc.* **1931**, 2213-2218.
- (20) Barclay, G. A.; Hoskins, B. F.; Kennard, C. H. L. *J. Chem. Soc.* **1963**, 5691-5699.
- (21) Murtha, D. P.; Walton, R. A. *Inorg. Chem.* **1973**, *12*, 368-372.
- (22) Burrstall, F. H.; Nyholan, R. S. *J. Chem. Soc.* **1952**, 3570-3579.

Table II. Positive Ion Spectra of 2,2'-Bipyridine and *o*-Phenanthroline Complexes^a

no.	compd	rel intens ^b					other ions (mass, rel intens)
		ML ₃ ⁺	ML ₂ X ⁺	ML ₂ ⁺	MLX ⁺	ML ⁺	
1	[Ag(bpy) ₂]NO ₃	c		17 (419)		100 (263)	43 (157) (2L + H) ⁺ (313, 40)
2	[Ag(<i>o</i> -phen) ₂]NO ₃			41 (467)		100 (287)	90 (181) (2L + H) ⁺ (313, 18)
3	[Cu(bpy) ₂]SO ₄			8 (375)		100 (219)	59 (157) (2L + H) ⁺ (313, 18)
4	[Cu(dmp) ₂]SO ₄ ·5H ₂ O			67 (479)		100 (271)	85 (209)
5	[Cu(<i>o</i> -phen) ₂]SO ₄ ·5H ₂ O			50 (423)		100 (243)	41 (181)
6	[Ti(<i>o</i> -phen) ₂](ClO ₄) ₂	6 (745)		81 (565)		100 (385)	2 (181) (2L + H) ⁺ (361, 24), (3L + H) ⁺ (541, 3)
7	[Fe(<i>o</i> -phen) ₃](ClO ₄) ₂	16 (596)	20 (515)	27 (416)		15 (236)	30 (181) FeL ₃ ClO ₄ ⁺ (695, 15), FeL ₃ ClO ₃ ⁺ (679, 8), FeL ₂ ClO ₄ ⁺ (499, 14), FeL ₂ Cl ⁺ (451, 11), FeL ₂ O ⁺ (432, 51), (2L + H) ⁺ (361, 100), FeLClO ₃ ⁺ (319, 77)
8	[Ni(bpy) ₃](ClO ₄) ₂	4 (526)	10 (469)	70 (370)	100 (313)	100 (214)	41 (157) NiL ₃ O ⁺ (542, 6), NiL ₂ O ⁺ (386, 100), (2L + H) ⁺ (313, 100), NiLCl ⁺ (249, 51)
9	[Ru(bpy) ₃]Cl ₂	9 (570)	100 (449)	96 (414)	6 (293)		100 (157) RuL ₂ Cl ₂ ⁺ (484, 62), RuLCl ₂ ⁺ (328, 13), (2L + H) ⁺ (313, 41)
10	[Co(<i>o</i> -phen) ₃]Cl ₂	7 (599)	8 (454)	100 (419)	100 (274)	44 (239)	40 (181)
11	[Ni(<i>o</i> -phen) ₃]Cl ₂	16 (598)	11 (453)	100 (418)	75 (273)	100 (238)	65 (181)
12	[Ni(bpy) ₃]X ₂ (a) X = Cl ⁻ (b) X = Br ⁻ (c) X = I ⁻ (d) X = NCS ⁻	2 (526)	10 (405)	85 (370)	65 (249)	100 (214)	88 (157)
		2 (526)	1 (449)	47 (370)	75 (295)	100 (214)	60 (157) (2L + H) ⁺ (313, 3)
		1 (526)	3 (497)	100 (370)	100 (341)	100 (214)	90 (157)
		3 (526)		19 (370)	26 (272)	100 (214)	89 (157)
13	[Mn(bpy) ₃]Br ₂		10 (446)		100 (290)	7 (211)	93 (157) (2L + H) ⁺ (313, 70)

^a Only ions corresponding to Na⁺, K⁺, and M⁺ (metal cation) are observed in the lower mass ranges. *m/z* ≤ (L + H)⁺; spectra were obtained near threshold energy. ^b Intensities as percent of base peak; peak masses are given in parentheses. ^c Ions were not detected.

Table III. Negative Ion Spectra of Coordination Compounds^a

compd	ions obsd	
	ions obsd	ions obsd
[AgL ₂]NO ₃	Ag(NO ₃) ₂ ⁻ NO ₃ ⁻	OCN ⁻
	100 (231) 99 (62)	CN ⁻
	24 (231) 100 (62)	5 (26)
		4 (26)
[M(<i>o</i> -phen) ₂ (H ₂ O) ₄](ClO ₄) ₂	M(ClO ₄) ₃ ⁻ ClO ₄ ⁻	Cl ⁻
2- <i>o</i> -phen	31 (435) 100 (99)	10 (35) 39 (26)
	7 (505) 100 (99)	6 (35) 67 (26)
[M(<i>o</i> -phen) ₃]Cl ₂	MCl ₃ ⁻ MCl ₂ CN ⁻	MCl ₂ ⁻ M(CN) ₂ ⁻ C ₃ N ⁻ Cl ⁻ CN ⁻
	31 (163) 5 (154)	85 (128) 100 (119) 40 (110) 13 (50) 27 (35) 21 (26)
	100 (164) 31 (155)	35 (129) 17 (120) 4 (111) 12 (50) 31 (35) 33 (26)
[M(bpy) ₃]Br ₂	MnBr ₃ ⁻ MnBr ₂ CN ⁻	C ₃ N ⁻ CN ⁻
	96 (294) 21 (241)	78 (50) 89 (26)
[Ru(bpy) ₃]Cl ₂	RuCl ₄ ⁻ RuCl ₃ ⁻	Cl ⁻ CN ⁻
	100 (242) 63 (207)	30 (35) 17 (26)
[Cu(dmp) ₂]SO ₄ ·5H ₂ O	Cu ₂ (SO ₄) ₂ ⁻ Cu(HSO ₄) ₂ ⁻	HSO ₄ ⁻ SO ₃ ⁻ CN ⁻
	19 (381) 11 (257)	100 (115) 99 (97) 37 (80) 36 (26)
[Ni(bpy) ₃](ClO ₄) ₂	Ni(ClO ₄) ₃ ⁻ NiO(ClO ₄) ₂ ⁻	Ni(CN) ₂ ⁻ Ni(CN) ₂ ⁻ ClO ₄ ⁻ Cl ⁻ OCN ⁻ CN ⁻
	40 (355) 15 (272)	48 (119) 25 (110) 100 (99) 13 (83) 9 (35) 19 (42) 60 (26)
[Ni(bpy) ₃](SCN) ₂	Ni(SCN) ₃ ⁻ Ni(CNS) ₂ (CN) ⁻	Ni(CNS) ₂ ⁻ SCN ⁻ CN ⁻
	35 (232) 20 (200)	80 (174) 38 (110) 70 (58) 100 (26)

^a Spectra were obtained near threshold energy; ion masses are given in parentheses.

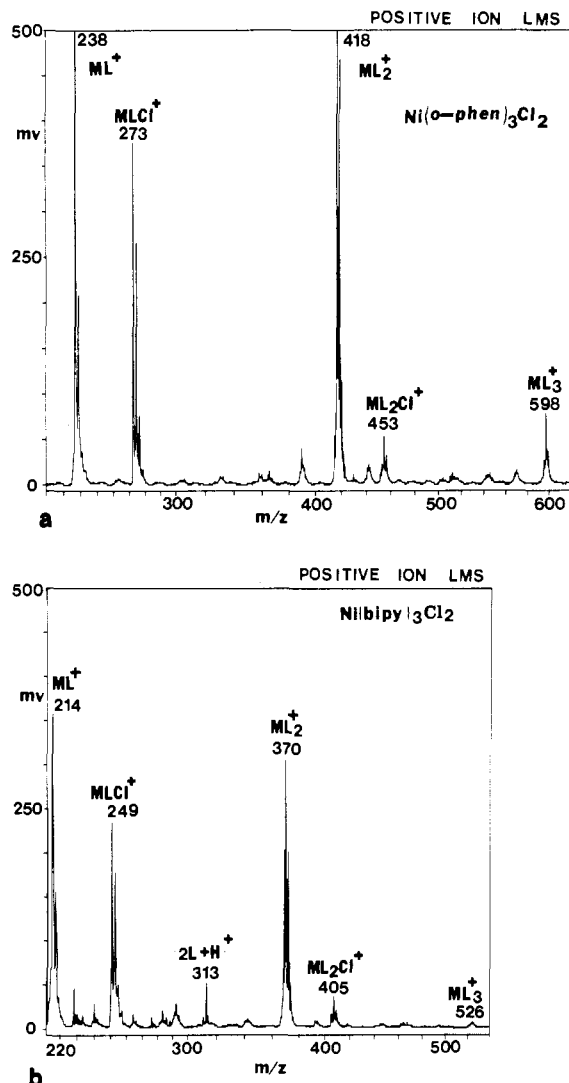


Figure 2. Positive ion laser mass spectra of $[\text{Ni}(\text{o-phen})_3]\text{Cl}_2$ (a) and $[\text{Ni}(\text{bpy})_3]\text{Cl}_2$ (b).

by normal fragmentation (Table II).

Hexacoordinate Complexes. The positive ion spectra of $[\text{Ni}(\text{o-phen})_3]\text{Cl}_2$ and $[\text{Ni}(\text{bpy})_3]\text{Cl}_2$ are shown in Figure 2 for the mass range $m/z > 200$; results for these and other hexacoordinate complexes are tabulated in Table II (7–13). The mass range $m/z < 200$ only shows ions corresponding to Na^+ , K^+ , M^+ (metal cation), and $(\text{L} + \text{H})^+$. In the mass range $m/z > 200$, ions corresponding to ML_3^+ , ML_2X^+ , ML_2^+ , MLX^+ , and ML^+ are observed for complexes such as $[\text{ML}_3]\text{X}_2$, where $\text{M} = \text{Co}$ and Ni and $\text{X} = \text{Cl}$, Br , and I . In the case of $[\text{Ru}(\text{bpy})_3]\text{Cl}_2$, ions corresponding to $\text{RuL}_2\text{Cl}_2^+$ and RuLCl_2^+ are also observed. Ions corresponding to $\text{Ni}_2\text{L}_2\text{S}^+$ and NiLCN^+ are observed in the positive ion spectrum of $[\text{Ni}(\text{bpy})_3](\text{NCS})_2$, in addition to the normal fragment ions NiL_3^+ , NiL_2^+ , NiL_2X^+ , and NiL^+ . No ions corresponding to ML_3^+ and ML_2^+ were observed in the positive ion spectrum of $[\text{Mn}(\text{bpy})_3]\text{Br}_2$; however, ions corresponding to ML_2X^+ , MLX^+ , and ML^+ are present (Table II).

The positive ion spectra of $[\text{Fe}(\text{o-phen})_3](\text{ClO}_4)_2$ and $[\text{Ni}(\text{bpy})_3](\text{ClO}_4)_2$ are different from those of other hexacoordinate complexes. The positive ion spectrum of $[\text{Fe}(\text{o-phen})_3](\text{ClO}_4)_2$ shows ions corresponding to $\text{FeL}_n\text{ClO}_3^+$ ($n = 1-3$), $\text{FeL}_3\text{ClO}_4^+$, FeL_2Cl^+ , and FeL_2O^+ , in addition to ML_3^+ , ML_2X^+ , ML_2^+ , and ML^+ , where $\text{X} = \text{ClO}_4^-$. In the case of $[\text{Ni}(\text{bpy})_3](\text{ClO}_4)_2$ (Figure 3), ions corresponding to NiL_3O^+ , NiL_2O^+ , and NiLCl^+ are detected along with NiL_3^+ , NiL_2X^+ , NiL_2^+ , NiLX^+ , and NiL^+ .

$[\text{M}(\text{o-phen})_2(\text{H}_2\text{O})_4](\text{ClO}_4)_2 \cdot 2\text{o-phen}$ ($\text{M} = \text{Ba}$, Pb). The positive ion spectra of these two complexes show ions corresponding to $\text{ML}_n\text{ClO}_4^+$ ($n = 2-4$), ML_nO^+ ($n = 2-3$), ML_nCl^+ ($n = 2-3$), ML^+ , $(2\text{L} + \text{H})^+$, $(\text{L} + \text{H})^+$, MCl^+ , MO^+ , and M^+ .

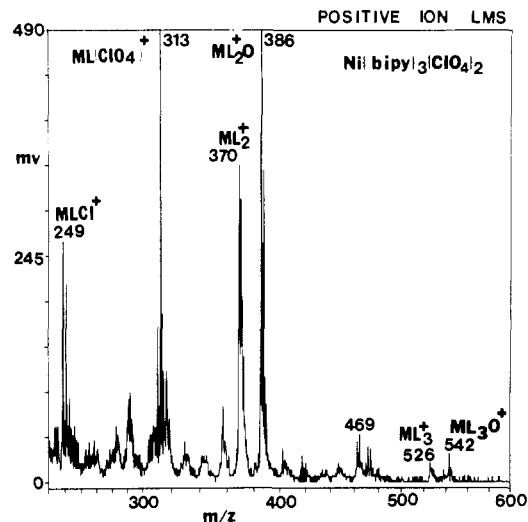


Figure 3. Positive ion laser mass spectrum of $[\text{Ni}(\text{bpy})_3](\text{ClO}_4)_2$.

Negative Ion Spectra. The ions observed in the negative ion LMS of the complexes studied are listed in Table III. The negative ion spectra of $[\text{Ag}(\text{bpy})_2]\text{NO}_3$ and $[\text{Ag}(\text{o-phen})_2]\text{NO}_3$ show ions corresponding to $\text{Ag}(\text{NO}_3)_2^-$, NO_3^- , OCN^- , and CN^- . Similarly, ions corresponding to $\text{M}(\text{ClO}_4)_3^-$, ClO_4^- , ClO_3^- , Cl^- , and CN^- are observed for $[\text{M}(\text{o-phen})_2(\text{H}_2\text{O})_4](\text{ClO}_4)_2 \cdot 2\text{o-phen}$ where $\text{M} = \text{Ba}$, Pb .

The negative ion spectra of $[\text{M}(\text{o-phen})_3]\text{Cl}_2$, where $\text{M} = \text{Ni}$ and Co , show similar ions corresponding to MCl_3^- , MCl_2CN^- , $\text{MCl}(\text{CN})_2^-$, MCl_2^- , MClCN^- , $\text{M}(\text{CN})_2^-$, C_3N^- , Cl^- , and CN^- (Table III). Negative ions observed for $[\text{Ni}(\text{bpy})_3]\text{X}_2$, where $\text{X} = \text{Cl}$, Br , and I , are very similar to those observed for $[\text{Ni}(\text{o-phen})_3]\text{Cl}_2$.

Ions corresponding to RuCl_4^- , RuCl_3^- , RuCl_2^- , Cl^- , and CN^- are observed in the case of $[\text{Ru}(\text{bpy})_3]\text{Cl}_2$. Except for the ion corresponding to $\text{NiO}(\text{ClO}_4)_2^-$, ions observed for $[\text{Ni}(\text{bpy})_3](\text{ClO}_4)_2$ are similar to those observed for $[\text{Ni}(\text{o-phen})_3]\text{Cl}_2$ (Table III).

Discussion

Tetracoordinate Complexes. The positive ion spectra of both silver complexes studied (Figure 1) are relatively simple; an intense peak is observed for AgL_2^+ ($\text{L} = \text{bpy}$ or o-phen). Fragmentation of silver complexes produces ions corresponding to AgL^+ and $(\text{L} + \text{H})^+$, which are useful for structure elucidation. Thus, the ions observed for these complexes are characteristic of their composition. The only significant difference between the two spectra shown in Figure 1 is an ion corresponding to $(2\text{L} + \text{H})^+$ for $[\text{Ag}(\text{bpy})_2]\text{NO}_3$; the $(2\text{L} + \text{H})^+$ ion is common for all 2,2'-bipyridine complexes studied.

The lower mass range ($m/z < 150$) for all tetracoordinate complexes is very simple; only sodium ($m/z = 23$), potassium ($m/z = 39, 41$), and the appropriate metal ions are observed. Thus, except for the ion corresponding to $(2\text{L} + \text{H})^+$, the spectra of $[\text{Ag}(\text{o-phen})_2]\text{NO}_3$ and $[\text{Ag}(\text{bpy})_2]\text{NO}_3$ show only the intact cation (AgL_2^+) and peaks that are structurally significant (AgL^+ , $(\text{L} + \text{H})^+$, and Ag^+). It is interesting to note that a peak corresponding to AgL_2^+ was not observed for $[\text{Ag}(\text{bpy})_2]\text{NO}_3$ using SIMS,¹³ though it was observed for $[\text{Ag}(\text{o-phen})_2]\text{NO}_3$.

The cation ML_2^+ was observed for all tetracoordinate complexes studied, regardless of the central metal ion. The other peaks in the spectra are similar to those observed for the silver complexes. For example, the positive ion LMS spectra of $[\text{Cu}(\text{dmp})_2]\text{SO}_4 \cdot 5\text{H}_2\text{O}$ and $[\text{Cu}(\text{bpy})_2]\text{SO}_4$ show ions corresponding to CuL_2^+ , CuL^+ , $(\text{L} + \text{H})^+$, and Cu^+ (Table II). The silver and copper complexes have different structures;²³ however, all show similar fragmentation patterns.

(23) Bailar, J. C., Jr.; Emeleus, H. J.; Nyholm, R.; Trotman-Dickenson, A. F., "Comprehensive Inorganic Chemistry"; Pergamon Press: Oxford, England, 1970; Vol. 3, pp 1-128.

The results obtained for *o*-phenanthroline and 2,2'-bipyridine complexes can be correlated with their solution stability constants. For example, the relative intensity of $\text{Ag}(\text{o-phen})_2^+$ (with respect to the base peak at $m/z > 150$) in the positive ion spectrum of $[\text{Ag}(\text{o-phen})_2]\text{NO}_3$ ($\log \beta_2 = 13.4$)²⁴ is always higher than that of $\text{Ag}(\text{bpy})_2^+$ in the positive ion spectrum of $[\text{Ag}(\text{bpy})_2]\text{NO}_3$ ($\log \beta_2 = 8.9$)²⁴ where β is the overall solution stability constant for the complex. The intensity variations of the other ions in the positive ion LMS of tetracoordinated complexes can also be explained using solution stability constants, as discussed above. The intensities of ML^+ ions are higher than those of ML_2^+ , an observation consistent with stability constants;^{24,26} the stability constant k_1 for ML^+ formation is greater than k_2 for ML_2^+ formation.

The positive ion spectrum of $[\text{Tl}(\text{o-phen})_2]\text{ClO}_4$ is similar to those of the silver and copper complexes, except that an ion corresponding to TlL_3^+ is observed (see Table II). TlL_3^+ ions are observed consistently at high laser powers; at lower laser powers near to threshold, TlL_3^+ ions are observed only once in about four to five laser firings (a complete spectrum is obtained from each laser firing). The stability constant for $[\text{Tl}(\text{o-phen})_2]^+$ reported from the literature²⁴ is small ($\log \beta_2 = 4$). Thus, $[\text{Tl}(\text{o-phen})_2]^+$ can decompose readily. Formation of TlL_3^+ corresponds to an ion-molecule reaction. It is possible that it arises from reaction of a free ligand with TlL_2^+ , $\text{TlL}_2^+ + \text{L} \rightleftharpoons \text{TlL}_3^+$, or by transfer of a ligand between two cations in the internal photoionization event, $2\text{TlL}_2^+ \rightleftharpoons \text{TlL}_3^+ + \text{TlL}^+$. The latter process is quite reasonable because of the size of Tl^+ ions (1.54 Å),²⁵ their vacant orbitals (5f, 6p, 6d), and the low stability of the Tl complex. However, the presence of peaks corresponding to $(n\text{L} + \text{H})^+$, where $n = 1-3$, tends to argue for direct ligand addition. On the basis of the present data, it is not possible to distinguish between the two possibilities.

Hexacoordinate Complexes. The highest mass ions detected for $[\text{NiL}_3]\text{Cl}_2$ complexes ($\text{L} = \text{o-phen}$ or bpy) (Figure 2) correspond to the molecular cation NiL_3^+ . The relative intensity of NiL_3^+ (with respect to the strongest peak at $m/z > 150$) in the positive ion LMS spectrum of $[\text{Ni}(\text{o-phen})_3]\text{Cl}_2$ is always higher than that for $[\text{Ni}(\text{bpy})_3]\text{Cl}_2$. The above observation agrees with the solution stability constants reported for $[\text{Ni}(\text{o-phen})_3]\text{Cl}_2$ ($\log \beta_3 = 24.7$)²⁶ and $[\text{Ni}(\text{bpy})_3]\text{Cl}_2$ ($\log \beta_3 = 20.2$).²⁶ The relative intensities of the ions corresponding to NiL^+ , NiL_2^+ , and NiL_3^+ decrease in the following order for the above two complexes:



This again agrees with the individual stability constants²⁶ from solution chemistry where $k_1 > k_2 > k_3$ for both complexes. Comparison of the positive ion spectrum of $[\text{Co}(\text{o-phen})_3]\text{Cl}_2$ ($\log \beta_3 = 19.90$)²⁶ with that of $[\text{Ni}(\text{o-phen})_3]\text{Cl}_2$ shows the intensity of NiL_3^+ is higher than that of CoL_3^+ , which again correlates with the stability constants: $\beta_3(\text{Ni analogue}) > \beta_3(\text{Co analogue})$. Thus, it seems to be that, in general, the relative intensities of various ions in the positive ion spectra can be correlated with the stability constants from solution chemistry. However, there are some exceptions. For example, in the case of $[\text{Ru}(\text{bpy})_3]\text{Cl}_2$ and $[\text{Fe}(\text{o-phen})_3](\text{ClO}_4)_2$, intensities of ions corresponding to ML_2^+ are greater than those corresponding to ML^+ or ML_3^+ . Stability constant data are not available for $[\text{Ru}(\text{bpy})_3]\text{Cl}_2$ to rationalize the above observation. In the case of $[\text{Fe}(\text{o-phen})_3](\text{ClO}_4)_2$, the stability constants for the individual steps follow the order $k_3 > k_2 > k_1$,²⁴ inconsistent with the greater intensity of ML_2^+ relative to ML_3^+ . Thus, one should exercise some caution in using stability constant data to predict intensity variations in the LMS of coordination complexes.

All compounds other than tetracoordinate complexes show ions corresponding to ML_2X^+ and MLX^+ ($\text{X} = \text{monovalent anion}$)

in addition to ML_3^+ , ML_2^+ , and ML^+ . The production of ML_2X^+ and MLX^+ ions by internal decomposition is quite reasonable, because addition/association of X^- to ML_n^{2+} (hexacoordinate complexes) will lead to charged species such as ML_nX^+ , since the metal atom in the original complex is formally in a +2 oxidation state. On the other hand, since the central metal atom in the original tetracoordinate complex is formally in a +1 oxidation state, addition/association of X^- to species such as ML_n^+ will produce neutral species that cannot be detected. The above may be the reason for the absence of ions corresponding to ML_2X^+ and MLX^+ in the case of tetracoordinate complexes. The formation of ML_2X^+ and MLX^+ (hexacoordinate complexes) may be also facilitated by Coulombic attraction between species such as ML_n^{2+} ($n = 1-2$) and X^- and vacant d orbitals in the central metal atom.

Most fragmentation patterns of the complexes discussed so far resemble each other within a group (e.g., tetracoordinated, hexacoordinated). However, a few compounds represent exceptions. For example, in the positive ion LMS spectrum of $[\text{Mn}(\text{bpy})_3]\text{Br}_2$, no ions corresponding to ML_3^+ or ML_2^+ were observed; ions corresponding to ML^+ are weak. However, strong peaks are observed for ions corresponding to MnLBr^+ and MnL_2Br^+ (Table II). $[\text{Mn}(\text{bpy})_3]\text{Br}_2$ is less stable than the other complexes ($\log \beta_3 = 5.9$)²⁶ and readily loses a ligand in aqueous solutions.²⁷ Thus, the low stability constants ($\log k_1 = 2.55$, $\log k_2 = 1.9$, and $k_3 = 1.45$)²⁶ correlate with failure to observe ions corresponding to ML_3^+ and ML_2^+ . Because of Coulombic attractions, ions corresponding to MnL_2Br^+ and MnLBr^+ are probably more stable than ions such as MnL_3^+ and MnL_2^+ . Thus, it appears that a complex having a small value for its stability constant $[\text{Mn}(\text{bpy})_3]\text{Br}_2$ will follow a different fragmentation pattern compared with relatively stable complexes.

Although the central metal atom is formally in a +2 oxidation state in all original compounds except for the tetracoordinate complexes, no doubly charged or multicharged cations were observed in the LMS spectra. In the case of nickel complexes, nickel is formally reduced to the +1 oxidation state in species such as NiL_3^+ , NiL_2^+ , and NiL^+ ; in ions like NiL_2Cl^+ and NiLCl^+ , nickel is formally in a +2 oxidation state. Although formal reduction of metal cation is observed for all complexes, formal oxidation of the metal cation to a higher state is not observed except for $[\text{Ru}(\text{bpy})_3]\text{Cl}_2$. The positive ion spectrum of $[\text{Ru}(\text{bpy})_3]\text{Cl}_2$ shows ions corresponding to $\text{RuL}_2\text{Cl}_2^+$ and RuLCl_2^+ , in addition to RuL_3^+ , RuL_2^+ , and RuL_2Cl^+ . Ruthenium is formally in a +3 oxidation state in species such as $\text{RuL}_2\text{Cl}_2^+$ and RuLCl_2^+ . It has been shown that $[\text{Ru}(\text{bpy})_3]^{2+}$ can undergo photochemical oxidation by absorption of UV radiation.²⁸ Thus, the observation of ions corresponding to $\text{RuL}_2\text{Cl}_2^+$ and RuLCl_2^+ may result from photooxidation of $[\text{Ru}(\text{bpy})_3]\text{Cl}_2$. The species $[\text{Ru}(\text{bpy})_2\text{Cl}_2]^+$ is known in solution chemistry;²⁹ the observation of $[\text{Ru}(\text{bpy})_2\text{Cl}_2]^+$ in the LMS spectrum indicates that it is also stable in the gas phase. Thus, it appears again that, at least qualitatively, stable species in LMS spectra can be correlated with the solution stability of transition-metal complexes.

Effect of Anion on Ion Production. A series of nickel complexes $[\text{Ni}(\text{bpy})_3]\text{X}_2$ ($\text{X} = \text{Cl}^-$, Br^- , ClO_4^- , SCN^-) was studied to investigate the effect of the anion on ion production in LMS.

The positive ion spectra of the halide ($\text{X} = \text{Cl}^-$, Br^- , I^-) complexes show similar fragmentation patterns. In contrast, the positive ion spectra of $[\text{Ni}(\text{bpy})_3](\text{ClO}_4)_2$ and $[\text{Ni}(\text{bpy})_3](\text{SCN})_2$ show different fragmentation behavior. As observed for the halide analogues, ions corresponding to NiL_3^+ , NiL_2X^+ , NiL_2^+ , and NiLX^+ , where $\text{X} = \text{ClO}_4^-$, are observed in the positive ion LMS spectrum of $[\text{Ni}(\text{bpy})_3](\text{ClO}_4)_2$ (Figure 3). Also, ions are seen corresponding to NiL_3O^+ , NiL_2O^+ , and NiLCl^+ , which are more intense than NiL_3^+ and NiL_2^+ . The results obtained for $[\text{Fe}(\text{o-phen})_3](\text{ClO}_4)_2$ are very similar to those for $[\text{Ni}(\text{bpy})_3](\text{ClO}_4)_2$;

(24) See ref 1; Chapter II.

(25) Lee, A. G. *Coord. Chem. Rev.* **1972**, *8*, 289-349.

(26) McBryde, W. A. E. "A Critical Review of Equilibrium Data for Proton and Metal Complexes of 1,0-Phenanthroline, 2,2'-Bipyridyl and Related Compounds"; Pergamon Press: Oxford, England, 1978.

(27) See ref 23; pp 771-786.

(28) Kalyanasundaram, K. *Coord. Chem. Rev.* **1982**, *46*, 159-244.

(29) Miller, R. R.; Brandt, W. W., Sr.; Marina Puke, O. S. F. *J. Am. Chem. Soc.* **1955**, *77*, 3178-3180.

ions corresponding to $\text{FeL}_3\text{ClO}_4^+$, $\text{FeL}_n\text{ClO}_3^+$ ($n = 1-3$), FeL_2O^+ , and FeL_2Cl^+ are observed, in addition to the ions from normal fragmentation. Iron and nickel are formally in a +3 oxidation state in ML_nO^+ ($M = \text{Ni, Fe; } n = 2-3$), in a +2 oxidation state in ML_nX^+ ($M = \text{Ni, Fe; } n = 1-3$; $\text{X} = \text{ClO}_4^-, \text{ClO}_3^-, \text{Cl}^-$) and in a +1 oxidation state in ML_n^+ ($n = 1-3$).

In a recent study in our laboratory it was noticed that ligands such as *o*-phenanthroline and 2,2'-bipyridine undergo ion-molecule reactions in the presence of NaNO_3 , leading to $(\text{M} + \text{O} - \text{H})^-$ ions in the negative ion spectra. Thus, one possibility to explain the presence of species such as NiL_3O^+ , NiL_2O^+ , and FeL_2O^+ is the oxidation of ligands by ClO_4^- species leading to hydroxy-*o*-phenanthroline, rather than oxidation of the central metal atom. However, the absence of ions corresponding to $(\text{M} + \text{O} - \text{H})^-$ for the ligand in the negative ion LMS of $[\text{ML}_3](\text{ClO}_4)_2$ ($M = \text{Ni, L} = \text{bpy; } M = \text{Fe, L} = \textit{o}$ -phen) excludes the above possibility.

The above discussion indicates that ions corresponding to NiL_2O^+ , NiLO^+ , and FeL_2O^+ are probably produced by the oxidation of central metal atoms. The production of NiL_2O^+ , NiLO^+ , and FeL_2O^+ may take place either by internal decomposition or by an ion-molecule reaction. Direct reaction between ClO_4^- and the complex may lead to species such as NiL_3O^+ , NiL_2O^+ , NiLCl^+ , and ClO_3^- . The observation of NiL_3O^+ , NiL_2O^+ , NiLCl^+ , and ClO_3^- in the LMS spectrum of $[\text{Ni}(\text{bpy})_3](\text{ClO}_4)_2$ tends to support internal decomposition of the complex as a mechanism. The idea of internal decomposition is further supported by the observation of ions corresponding to $\text{NiO}(\text{ClO}_4)_2^-$ in the negative ion LMS spectrum of $[\text{Ni}(\text{bpy})_3](\text{ClO}_4)_2$. The possibility of reactions between O^- or O_2^- and the complex leading to NiL_3O^+ and NiL_2O^+ can be excluded since no ions corresponding to O^- or O_2^- were observed in the negative ion spectra of any complex. Thus, the presence of NiL_3O^+ and NiL_2O^+ in the positive ion LMS spectrum and the absence of O^- or O_2^- in the negative ion LMS spectrum of $[\text{Ni}(\text{bpy})_3](\text{ClO}_4)_2$ tend to support internal decomposition rather than ion-molecule reactions. Ions corresponding to NiL_3O^+ and NiL_2O^+ are probably stable, since synthesis and existence of Ni and Fe compounds in higher oxidation states ($\text{NiO}(\text{OH})$) $[\text{Ni}(\text{en})_2\text{Cl}_2]\text{Cl}_2$ have been reported.³⁰

The positive ion LMS spectrum of $[\text{Ni}(\text{bpy})_3](\text{NCS})_2$ shows ions corresponding to NiL_3^+ , NiL_2^+ , $\text{NiL}(\text{NCS})^+$, and NiL^+ from normal fragmentation; the spectrum is dominated by NiL^+ . In addition, ions corresponding to NiLCN^+ and $\text{Ni}_2\text{L}_2\text{S}^+$ are observed. Detection of species such as NiLCN^+ also supports internal decomposition.

Coordination Compounds Having More Than Three Ligands.

Two complexes were studied that are different from those discussed so far with respect to coordination: $[\text{M}(\textit{o}$ -phen)₂(H₂O)₄](ClO₄)₂·2*o*-phen, where $M = \text{Ba}$ and Pb . Although these complexes have four *o*-phenanthroline molecules per metal atom, only two are coordinated directly to the central metal ion.³¹ Generally, these complexes are regarded as eight-coordinated, because water molecules occupy the other four coordination sites.³¹ These complexes have exceptionally distorted cubic structures, and both the coordinated and uncoordinated *o*-phenanthroline molecules are packed in parallel planes.³¹

The positive ion spectrum of $[\text{Ba}(\textit{o}$ -phen)₂(H₂O)₄](ClO₄)₂·2*o*-phen is shown in Figure 4 for $m/z > 500$. The highest mass ion detected corresponds to $\text{BaL}_4(\text{ClO}_4)^+$. The observation of $\text{BaL}_4(\text{ClO}_4)^+$ requires that uncoordinated *o*-phenanthroline molecules substitute for water molecules in the LMS volatilization/ionization processes. This is further supported by the observation of ions corresponding to $\text{BaL}_3\text{ClO}_4^+$, $\text{BaL}_2\text{ClO}_4^+$, and BaL_3^+ . The formal intact cation corresponding to $[\text{Ba}(\textit{o}$ -phen)₂(H₂O)₄]⁺ is not observed. Ions corresponding to BaL_2O^+ ($m/z = 514$), BaL_3O^+ ($m/z = 694$), BaL_2Cl^+ ($m/z = 533$), and BaL_3Cl^+ ($m/z = 713$) (Figure 4) reflect the nature of the anion (ClO_4^-) present. In the lower mass ranges ions corresponding to

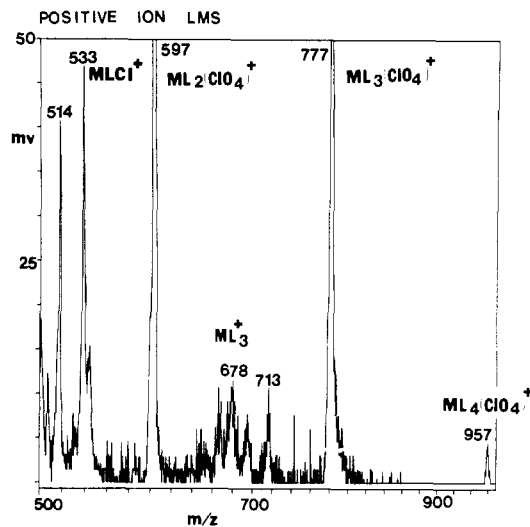


Figure 4. Positive ion laser mass spectrum of $[\text{Ba}(\textit{o}$ -phen)₂(H₂O)₄](ClO₄)₂·2*o*-phen.

BaO^+ ($m/z = 154$, 96%), BaCl^+ ($m/z = 173$, 50%), $(\text{L} + \text{H})^+$ ($m/z = 181$, 100%), BaL^+ ($m/z = 318$, 2%), and $(2\text{L} + \text{H})^+$ ($m/z = 361$, 14%) are detected. Ions such as MgO^+ , CaO^+ , and SrO^+ , which are similar to BaO^+ , have been also reported for MgO , CaO , and SrO in electron-impact mass spectrometry.³² BaO^+ can be formally considered to exist either in the form of Ba^{2+}O^- or Ba^+O rather than $\text{Ba}^{3+}\text{O}^{2-}$, since the third ionization potential for barium is very high. No species having barium in a +3 oxidation state was observed in the negative ion LMS of $[\text{Ba}(\textit{o}$ -phen)₂(H₂O)₄](ClO₄)₂·2*o*-phen, excluding the possibility that barium is formally in a +3 oxidation state in BaO^+ . This is reasonable because species having higher oxidation states were observed in the cases of Ru and Ni in the negative ion LMS spectra of $[\text{Ru}(\text{bpy})_3]\text{Cl}_2$ and $[\text{Ni}(\text{bpy})_3](\text{ClO}_4)_2$, respectively.

The important ions observed in the positive ion LMS spectrum of $[\text{Pb}(\textit{o}$ -phen)₂(H₂O)₄](ClO₄)₂·2*o*-phen correspond to $\text{PbL}_4(\text{ClO}_4)^+$ ($m/z = 1027$), $\text{PbL}_3\text{ClO}_4^+$ ($m/z = 847$), $\text{PbL}_2\text{ClO}_4^+$ ($m/z = 667$), PbL_2Cl^+ ($m/z = 603$), $(3\text{L} + \text{H})^+$ ($m/z = 541$), $(2\text{L} + \text{H})^+$ ($m/z = 361$), PbCl^+ ($m/z = 243$), Pb^+ ($m/z = 208$), PbL_3O^+ ($m/z = 764$), and PbL_2O^+ ; the spectrum is dominated by Pb^+ .

Negative Ion Spectra. The negative ion spectra of all complexes provide information about the oxidation state of the central ion in the original complexes and the anion present and evidence for internal decomposition. The highest mass ion detected in the negative spectrum of any complex generally corresponds to MX_{n+1}^- , where n is the oxidation state of the metal, if X is a monovalent anion (Table III).

Ions corresponding to $\text{RuL}_2\text{Cl}_2^+$ and RuLCl_2^+ in the positive ion LMS spectrum of $[\text{Ru}(\text{bpy})_3]\text{Cl}_2$ indicate oxidation of ruthenium from +2 (original compound) to +3 (LMS). This oxidation is confirmed by ions corresponding to RuCl_4^- in the negative ion LMS spectrum of $[\text{Ru}(\text{bpy})_3]\text{Cl}_2$. Thus, for $[\text{Ru}(\text{bpy})_3]\text{Cl}_2$, the highest ion mass detected (RuCl_4^-) in the negative ion spectra corresponds to a higher oxidation state (+3) for ruthenium than would be expected (+2). The above observation is consistent with the ease of photooxidation of Ru(+2). Caution should be exercised when the highest ion mass detected in the negative ion LMS spectra of complexes is used to deduce the oxidation state of the central metal ion.

The negative ion LMS spectra of all complexes studied show ions corresponding to the anion X^- . Other ions arising from the central metal and anion are detected in all spectra, regardless of the ligand present. For example, the negative ion spectra of $[\text{Ag}(\textit{o}$ -phen)₂NO₃] and $[\text{Ag}(\text{bpy})_2]\text{NO}_3$ show ions such as $\text{Ag}(\text{NO}_3)_2^-$, NO_3^- , NO_2^- , and CN^- (Table III); similar ions were

(30) Levason, W.; McAuliffe, C. A. *Coord. Chem. Rev.* **1974**, *12*, 151-184.

(31) Smith, G.; O'Reilly, E. J.; Kennard, C. H. L.; White, A. H. *J. Chem. Soc., Dalton Trans.* **1977**, 1184-1190.

(32) Drowart, J.; Exsteen, G.; Verhaegen, G. *Trans. Faraday Soc.* **1964**, *60*, 1920-1933.

observed in the negative ion LMS spectra of Ba and Pb complexes (Table III).

Evidence for processes corresponding to ion-molecule reactions is also observed in the negative ion LMS spectra of the complexes. For example, the negative ion LMS spectra of $[M(o\text{-phen})_3]Cl_2$ ($M = Co, Ni$) shows ions corresponding to MCl_2CN^- , MCl_2^- , C_3N^- , Cl^- , and CN^- (Table III); CN^- ions produced in the plasma react to yield mixed cluster ions. Similar species involving CN^- ions are also observed in the negative ion LMS spectrum of $[Cu(dmp)_2]_2SO_4 \cdot 5H_2O$ (Table III).

In short, the negative ion spectra are useful for obtaining information about the anions, other anions produced by ion-molecule reactions, and the oxidation state of the central metal ion of the complex; they also provide supporting evidence for internal decomposition.

Acknowledgment. We are grateful to Professor B. E. Douglas and Dr. S. K. Viswanadham for useful discussions. Support of this work by the Office of Naval Research is gratefully acknowledged.

Contribution from the Department of Chemistry,
Yale University, New Haven, Connecticut 06511

Paramagnetic Phosphine Shift Reagents. 2. Study of the Structures of (Substituted-allyl)palladium Complexes in Solution

J. W. Faller,* C. Blankenship, B. Whitmore, and S. Sena

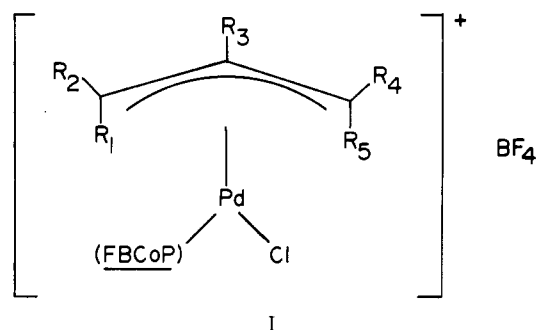
Received December 5, 1984

The use of a paramagnetic shift reagent analogue of a phosphine ligand for elucidation of the structures of (substituted-allyl)palladium complexes is described. Deuterium quadrupole splittings and isotropic shifts can be predicted from geometrical parameters based on model compounds. The magnetic susceptibility anisotropy is effectively constant within a series of complexes and allows predictions of shifts and/or geometry. Fitting of the data for a (η^3 -2-methylallyl)Pd complex required that the terminal protons be twisted out of the plane of the allyl carbon atoms. This twisting was confirmed by X-ray crystallographic analysis of a model compound, (η^3 -2-methylallyl)PdCl[P(C₆H₅)₃]. Crystal data: space group $P2_1/c$; $a = 11.931$ (4) Å; $b = 9.783$ (2) Å; $c = 17.286$ (6) Å; $\beta = 97.40$ (3)°; $V = 2001$ (2) Å³; $M_r = 459.25$; $Z = 4$; $\rho_{\text{calcd}} = 1.53$ g/cm³. For 2219 reflections ($F^2 \geq 3.0\sigma(F^2)$), $R_1 = 0.036$ and $R_2 = 0.040$.

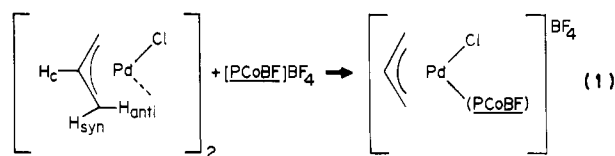
Paramagnetic shift reagents have been extensively studied with respect to the probing of geometry and conformation of substrates in solution.¹ Conventional reagents, such as lanthanide shift reagents, utilize the Lewis base affinity of metal ions for binding of substrates.² We recently reported³ the use of a shift reagent that possesses a phosphorus donor site capable of binding to Lewis acid centers and thereby allowing one to probe the structure of analogues of transition-metal complexes in solution. The exploitation of complexes that can be used as shift reagents, such as $[PCoBF]BF_4$ (see Figure 1), first prepared by Holm's group,^{4,5} is desirable owing to the ubiquitous presence of phosphine ligands in organometallics and the need to develop structural probes capable of characterizing catalytic intermediates in solution. We now report the synthesis and spectral characterization of a series of (substituted-allyl)palladium complexes of the general form shown in I.

Results and Discussion

The paramagnetic phosphine ligand is introduced into the palladium complex via the bridge-splitting reactions of the allylpalladium halide dimers (eq 1). The resulting palladium



- 1, $R_1 - R_5 = H$
 2, $R_1 = R_2 = R_3 = R_4 = H, R_5 = CH_3$
 3, $R_1 = R_2 = R_3 = R_5 = H, R_4 = CH_3$
 4, $R_1 = R_2 = R_3 = H, R_4 = R_5 = CH_3$
 5, $R_1 = R_3 = R_5 = H, R_2 = R_4 = CH_3$
 6a, $R_1 = R_2 = R_5 = H, R_3 = CH_3, R_4 = COCH_3$
 6b, $R_1 = R_2 = R_4 = H, R_3 = CH_3, R_5 = COCH_3$



- (1) Orrell, K. G. *Annu. Rep. NMR Spectrosc.* **1979**, *10*, 1 and references therein.
 (2) LaMar, G. N., Horrocks, W. D., Jr., Holm, R. H., Eds. "NMR of Paramagnetic Molecules"; Academic Press: New York, 1973.
 (3) Faller, J. W.; Blankenship, C.; Sena, S. *J. Am. Chem. Soc.* **1984**, *106*, 793-795.
 (4) Parks, J. E.; Wagner, B. E.; Holm, R. H. *Inorg. Chem.* **1971**, *10*, 2472-2478.
 (5) Larsen, E.; LaMar, G. N.; Wagner, B. E.; Parks, J. E.; Holm, R. H. *Inorg. Chem.* **1972**, *11*, 2652-2667.

complexes are all isolated as yellow air-stable solids, but undergo gradual decomposition in solution over several days. In the ¹H NMR spectra of the [(allyl)Pd(PCoBF)]BF₄ complexes, one observes that the resonances of the allylic ligands are shifted far downfield from the positions in their analogous diamagnetic dimers and triphenylphosphine complexes, as summarized in Tables I-III.

Assignment of Resonances. The resonances are assigned on the basis of their estimated relative distances and angles from the